

Hinode inversion strategy

Attacking inversion problems



PASJ: Publ. Astron. Soc. Japan **59**, S837–S844, 2007 November 30
© 2007, Astronomical Society of Japan.

Strategy for the Inversion of Hinode Spectropolarimetric Measurements in the Quiet Sun

David OROZCO SUÁREZ,¹ Luis R. BELLOT RUBIO,¹ Jose Carlos DEL TORO INIESTA,¹ Saku TSUNETE,²
Bruce LITES,³ Kiyoshi ICHIMOTO,² Yukio KATSUKAWA,² Shin'ichi NAGATA,⁴ Toshifumi SHIMIZU,⁵
Richard A. SHINE,⁶ Yoshinori SUEMATSU,² Theodore D. TARBELL,⁶ and Alan M. TITLE⁶

¹*Instituto de Astrofísica de Andalucía (CSIC), Apdo. de Correos 3004, 18080 Granada, Spain*
orozco@iaa.es

²*National Astronomical Observatory of Japan, 2-21-1 Osawa, Mitaka, Tokyo 181-8588*

³*High Altitude Observatory, National Center for Atmospheric Research, P.O. Box 3000, Boulder, CO 80307, USA*

⁴*Hida Observatory, Kyoto University, Kamitakara, Takayama, Gifu 506-1314*

⁵*Institute of Space and Astronautical Science, Japan Aerospace Exploration Agency, 3-1-1 Yoshinodai, Sagami-hara, Kanagawa 229-8510*

⁶*Lockheed Martin Solar and Astrophysics Laboratory, B/252, 3251 Hanover St., Palo Alto, CA 94304, USA*

(Received 2007 July 12; accepted 2007 September 11)

Abstract

In this paper we propose an inversion strategy for the analysis of spectropolarimetric measurements taken by Hinode in the quiet Sun. The Spectro-Polarimeter of the Solar Optical Telescope aboard Hinode records the Stokes spectra of the Fe I line pair at 630.2 nm with unprecedented angular resolution, high spectral resolution, and high sensitivity. We discuss the need to consider a *local* stray-light contamination to account for the effects of telescope diffraction. The strategy is applied to observations of a wide quiet Sun area at disk center. Using these data we examine the influence of noise and initial guess models in the inversion results. Our analysis yields the distributions of magnetic field strengths and stray-light factors. They show that quiet Sun internetwork regions consist mainly of hG fields with stray-light contamination of about 0.8.

Key words: instrumentation: high angular resolution — Sun: magnetic fields — Sun: photosphere

Why Hinode?

- spectra are easier to interpret than, e.g. CRISP (continuous WL coverage)
- straylight effects well studied (and understood)

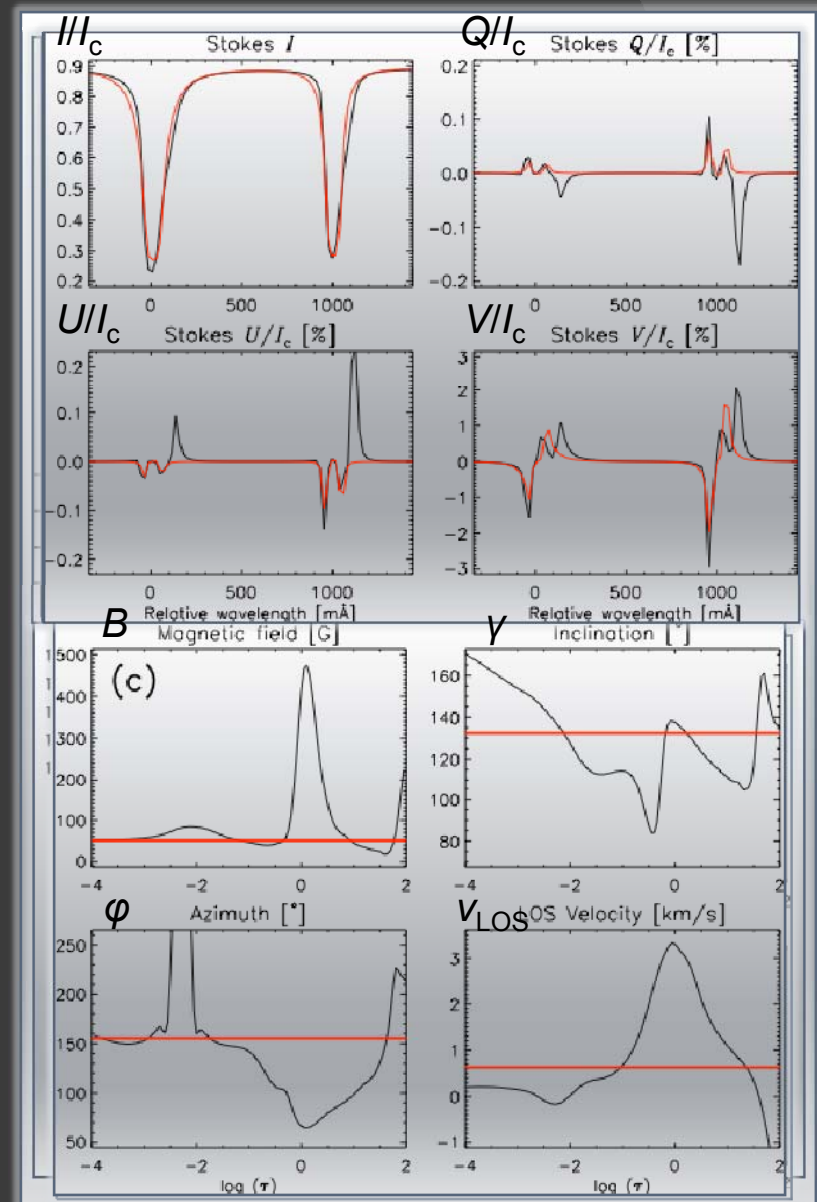
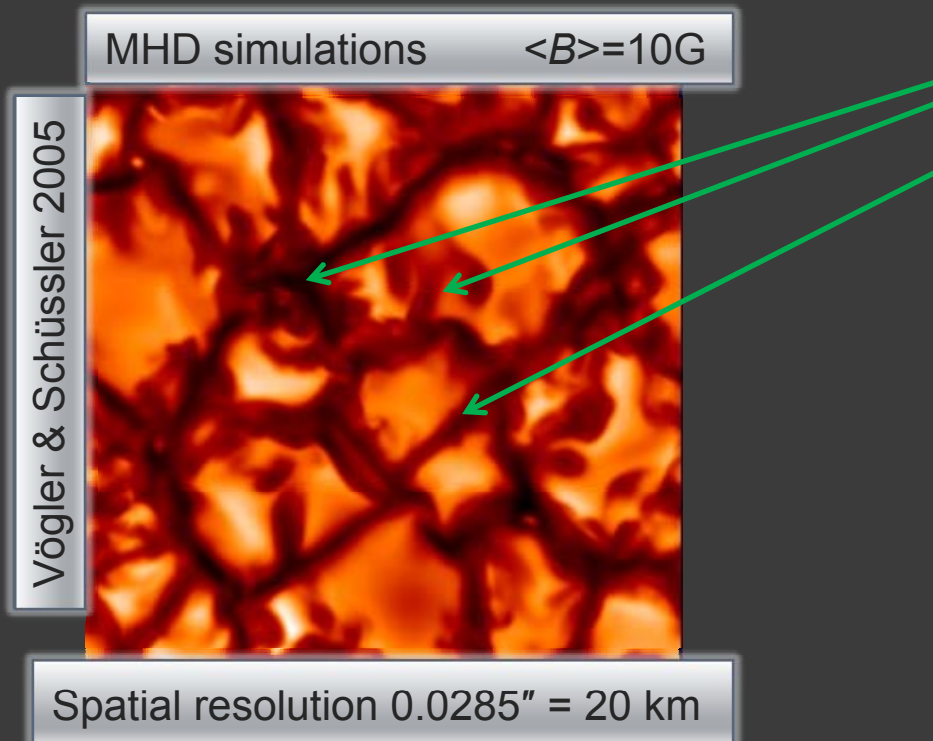
Why Quiet Sun?

- weak signals: ME appropriate approach
- interesting effects, especially concerning straylight

Hinode inversions

- ⊙ diffraction limited observations
 - ⊙ angular resolution $0.32''$ (limited by pixel size of $0.16''$)
 - ⊙ free from seeing effects
-
- light entering the telescope comes from a much smaller region than for ground based telescopes
 - results in significantly larger polarization signals
 - effect of noise is minimized
 - less atmospheric components mixed together in one resolution element
 - facilitates the interpretation of data
 - *allows for simpler atmospheric models*
 - *Milne-Eddington appropriate*
 - **CHECK using MHD!**

- Magnetohydrodynamic simulations of the quiet-Sun provides “realistic” model atmospheres: $\langle B \rangle = 10, 50, 140 \text{ G}$
- Fe I 630.15 and 630.25 nm spectral lines with no noise and not affected by the measurement process
- Wavelength sampling 2.15 nm



How to compare MHD and ME?

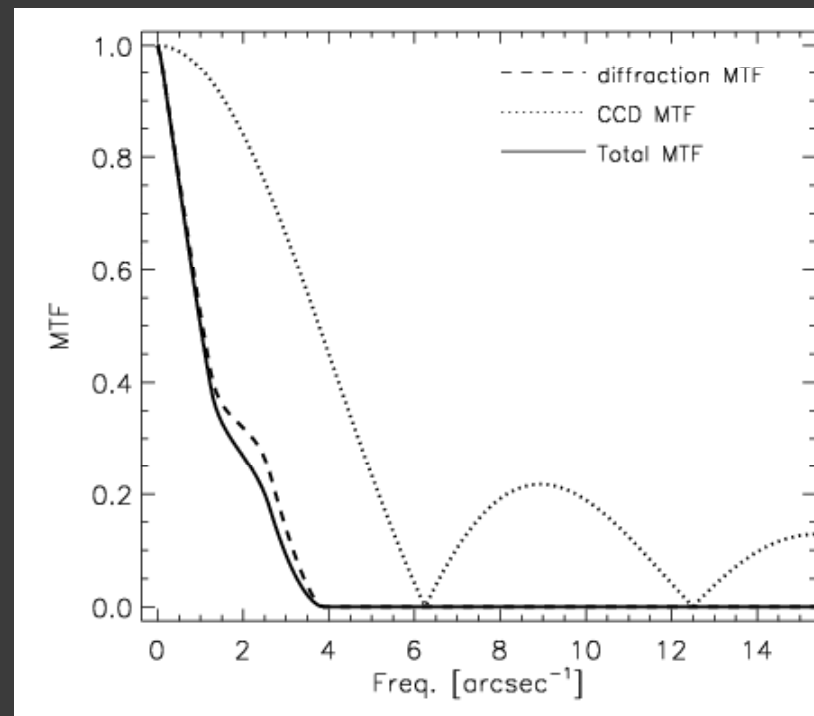
- Atmospheric quantities vary with height
- ME inversions provide single quantities that can be interpreted as averages of the real stratifications (Westendorp Plaza et al. 1998)
- Analytically, it is possible to determine the “height of formation of a ME measurements” (Sánchez Almeida et al. 1996)
- In practice this concept is of little use since the conditions of the atmosphere are not known
- The formation height is deeper in intergranular lanes than in granule centers
- ME inferences cannot be assigned to a constant optical depth layer
- The height at which the ME parameters refer to change depending on the physical parameter

Hinode measurements – spatial degradation

Hinode: 0.5 m telescope with spatial resolution $\sim 0.26''$ @ 630 nm
($\sim 190\text{km}$)

1. Degradation by telescope diffraction $\rightarrow \sim 0.26''$

Aperture	0.5 m
Working wavelength	630 nm
Spatial resolution	$\sim 0.26''$ $\sim 190\text{ km}$
Central obscuration	34.4%
CCD pixel size	$0.16'' \times 0.16''$



Study using MHD simulations

MHD (SOT/SP res.) degrade to SOT/SP

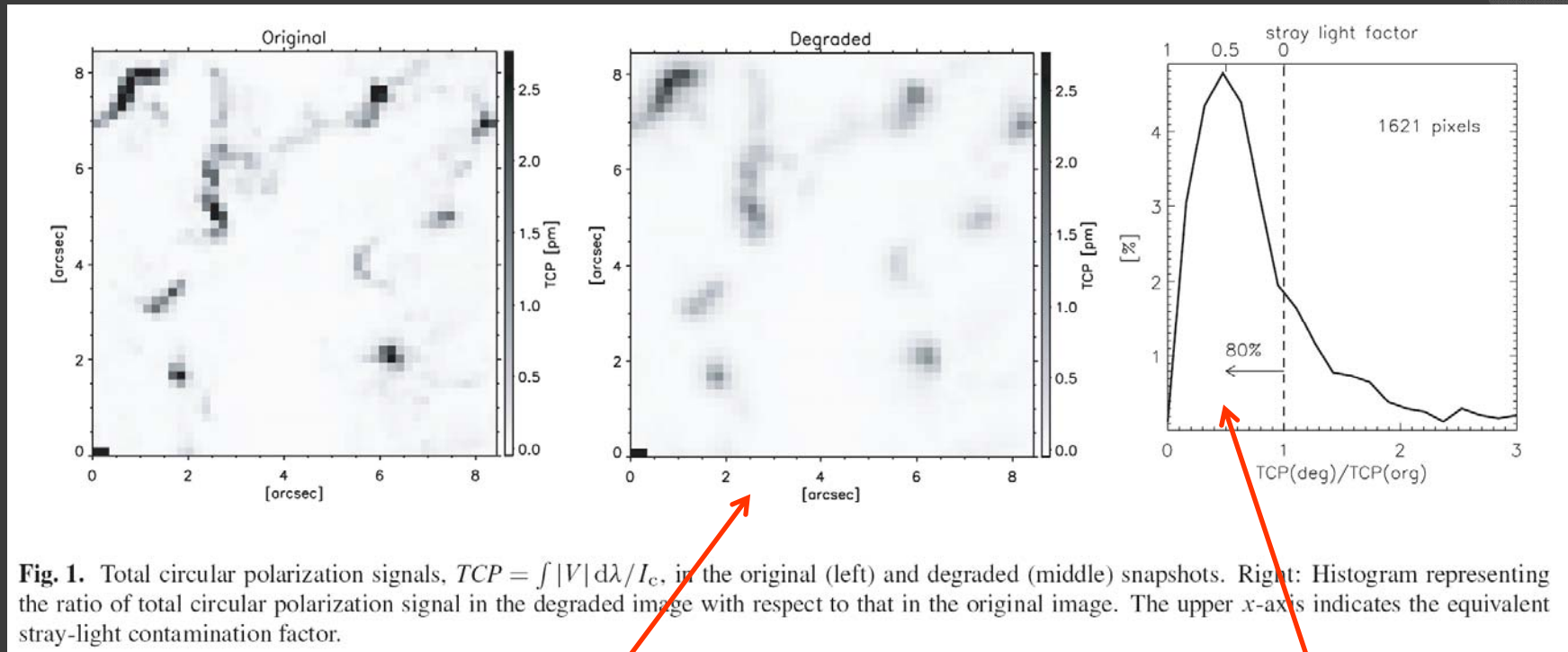


Fig. 1. Total circular polarization signals, $TCP = \int |V| d\lambda / I_c$, in the original (left) and degraded (middle) snapshots. Right: Histogram representing the ratio of total circular polarization signal in the degraded image with respect to that in the original image. The upper x-axis indicates the equivalent stray-light contamination factor.

substantial loss of contrast (15% \rightarrow 7.5%)

80% of blurred profiles show TCP lower than original

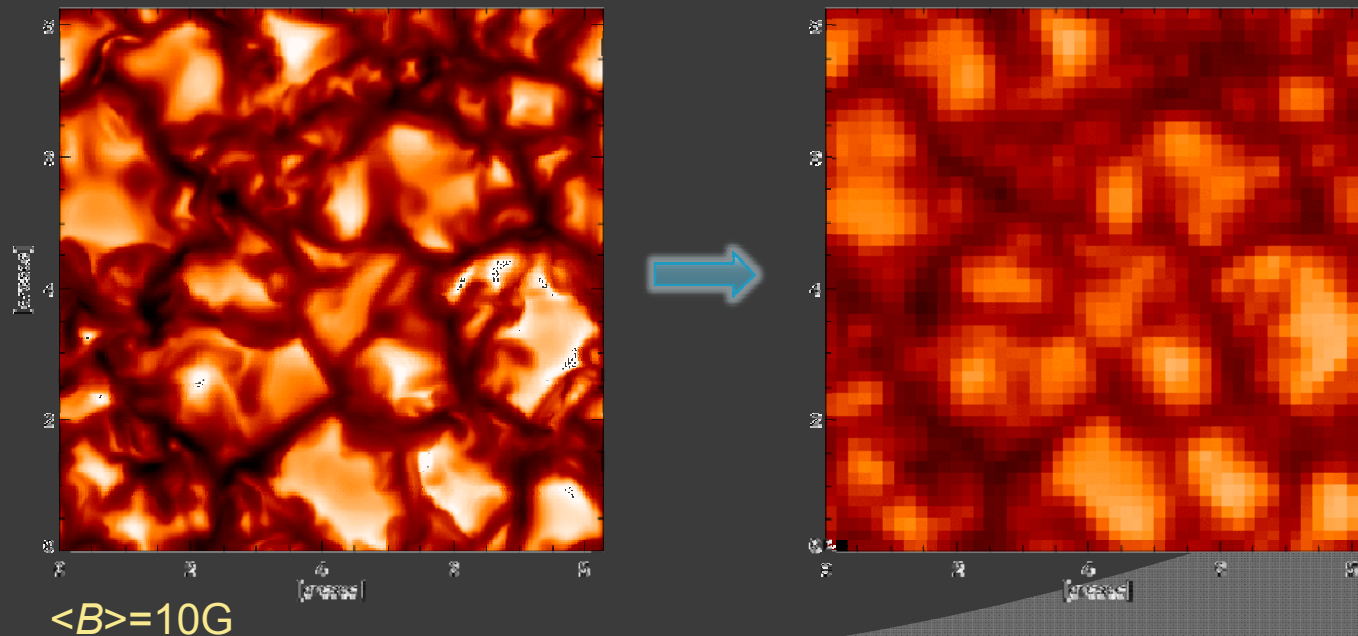
This decrease is not due to cancellation of opposite polarity fields, but a true result of the telescope diffraction.

\rightarrow It is important to include the stray/scattered light of the surrounding pixels (contamination factor)

Hinode measurements – spatial degradation

Hinode: 0.5 m telescope with spatial resolution $\sim 0.26''$ @ 630 nm
($\sim 190\text{km}$)

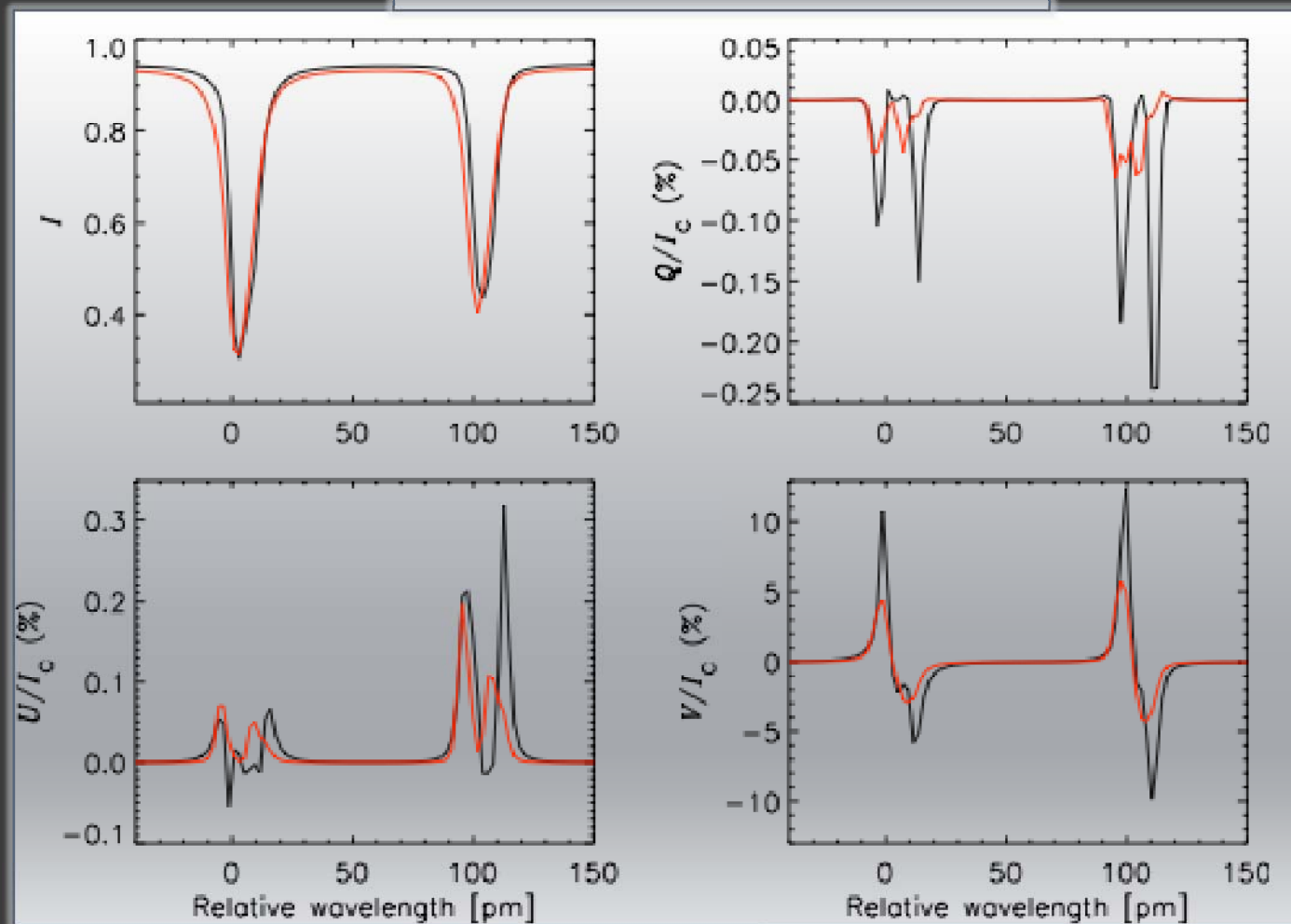
1. Degradation by telescope diffraction $\rightarrow \sim 0.26''$
2. Degradation by CCD pixel size $\rightarrow \sim 0.32''$
3. Reduction of rms contrast from 13.7% to 8.5% (the rms contrast of real *Hinode*/SP observations is $\sim 7.5\%$)



Telescope diffraction – effect on spectra

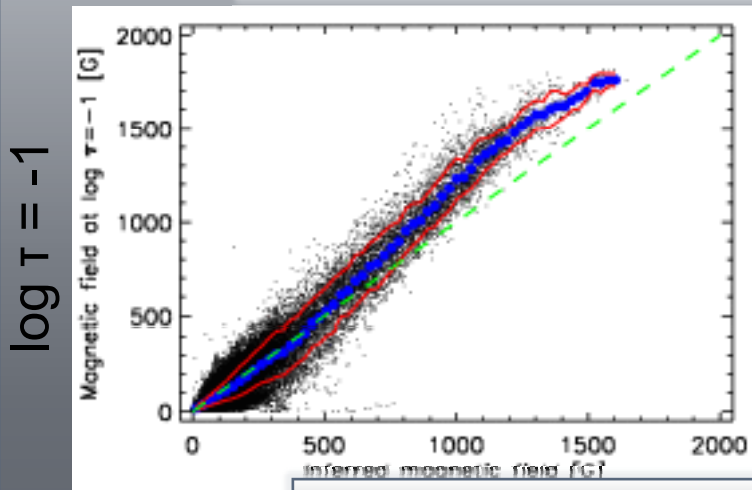
Telescope diffraction modifies the shape of the Stokes profiles

Black = before ; red = after

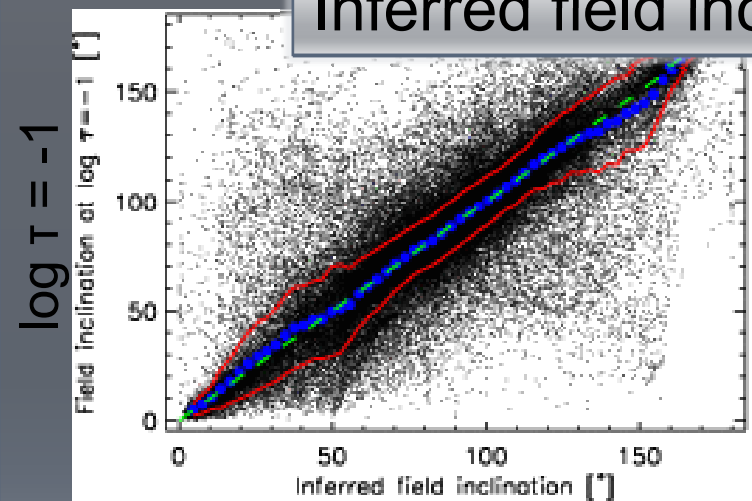


Quantitative analysis of ME performance

Inferred field strength



Inferred field inclination



Blue = mean ; red = rms

- Quantitative comparison with the real atmospheric parameters at $\log \tau = -1$
- The scatter is a combination of the use of a ME model atmosphere to fit asymmetric Stokes profiles and the pixel-to-pixel variations of the “height of formation”
- The deviation of the magnetic field strength from one-to-one correspondence is due to the variation of the height of formation in the magnetic field with the field strength

ME inferences of solar magnetic fields

- Conclusion: ME inversions provide good estimates of the physical quantities present at $\log \tau = -1$

Field strength	Inclination	Azimuth	LOS velocity
30 G	6°	20°	500 m/s

- Caution: These differences may be rather large for individual pixels even when the fit is good
→ do not trust individual pixels too much!
- The differences associated to the ME approximation dominate against those due to photon noise of the observations

(Orozco Suárez et al., in prep)

How to include straylight?

Global straylight:

- when telescope has wide PSF (pixel contains information also from regions far away)
 - seeing / AO induced wide PSF
- average quiet Sun profile as straylight component

Local straylight:

- narrow PSF (Hinode)
- average over I profile of neighboring pixels

Should the local straylight be polarized or unpolarized?

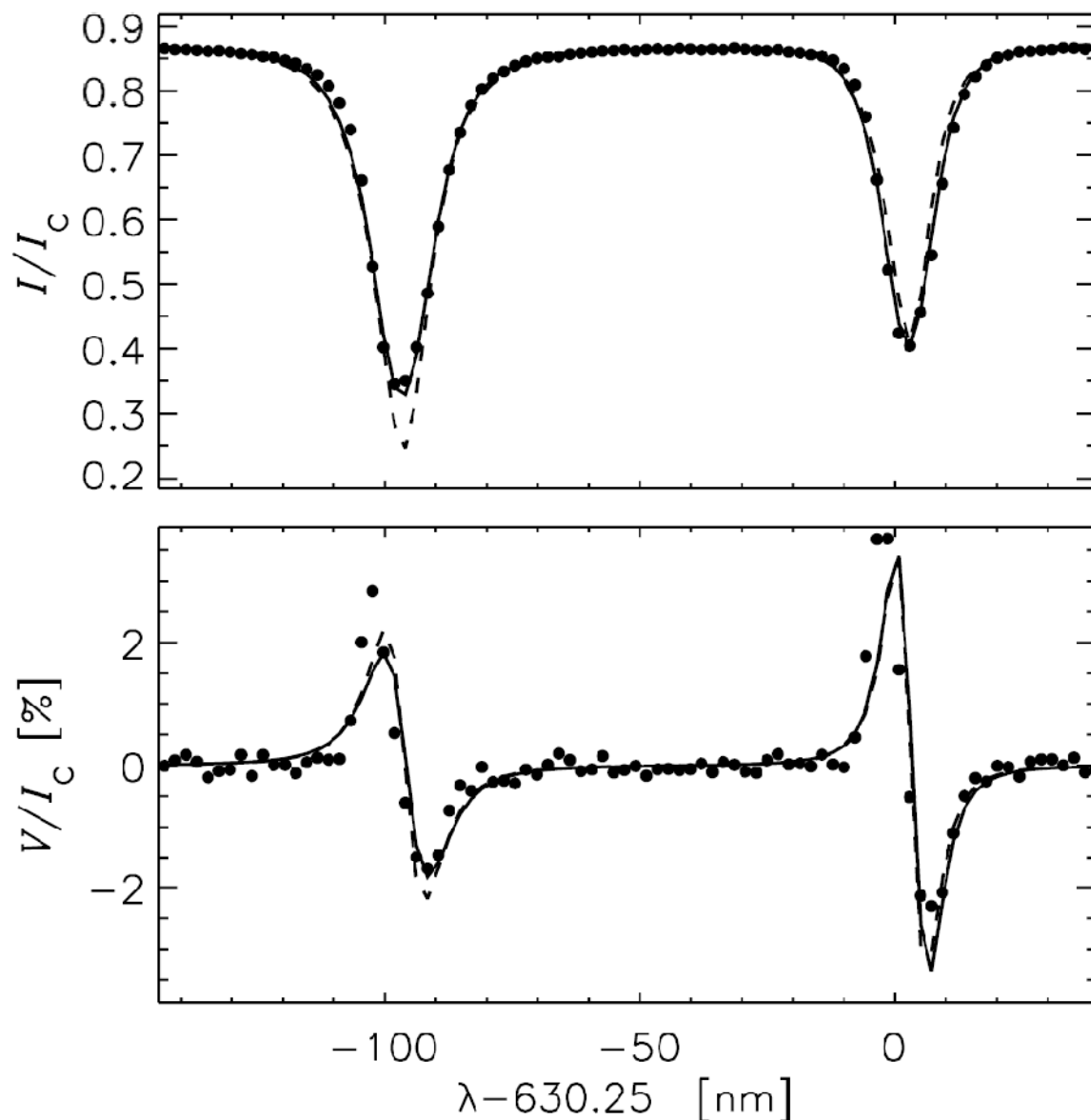


Fig. 2. Observed (dots) and best-fit Stokes I and V profiles from simulated Hinode/SP observations using a global (dashed), and a local (solid) stray-light profile contamination in the inversion.

- Invert the Stokes profiles assuming a homogeneous magnetic atmosphere occupying the whole resolution elements and a contamination of “*stray light*”
- The idea is to correct for the dilution of the polarization signals due to diffraction
- The “stray light” profile is evaluated individually for each pixel by averaging the Stokes / profiles within a 1"-wide box centered on the pixel
- 10 free parameters are determined (S_0 , S_1 , η_0 , $\Delta\lambda_D$, a , B , γ , χ , v_{LOS} , α)

This strategy represents a significant improvement over conventional treatments in which a global stray-light profile is considered

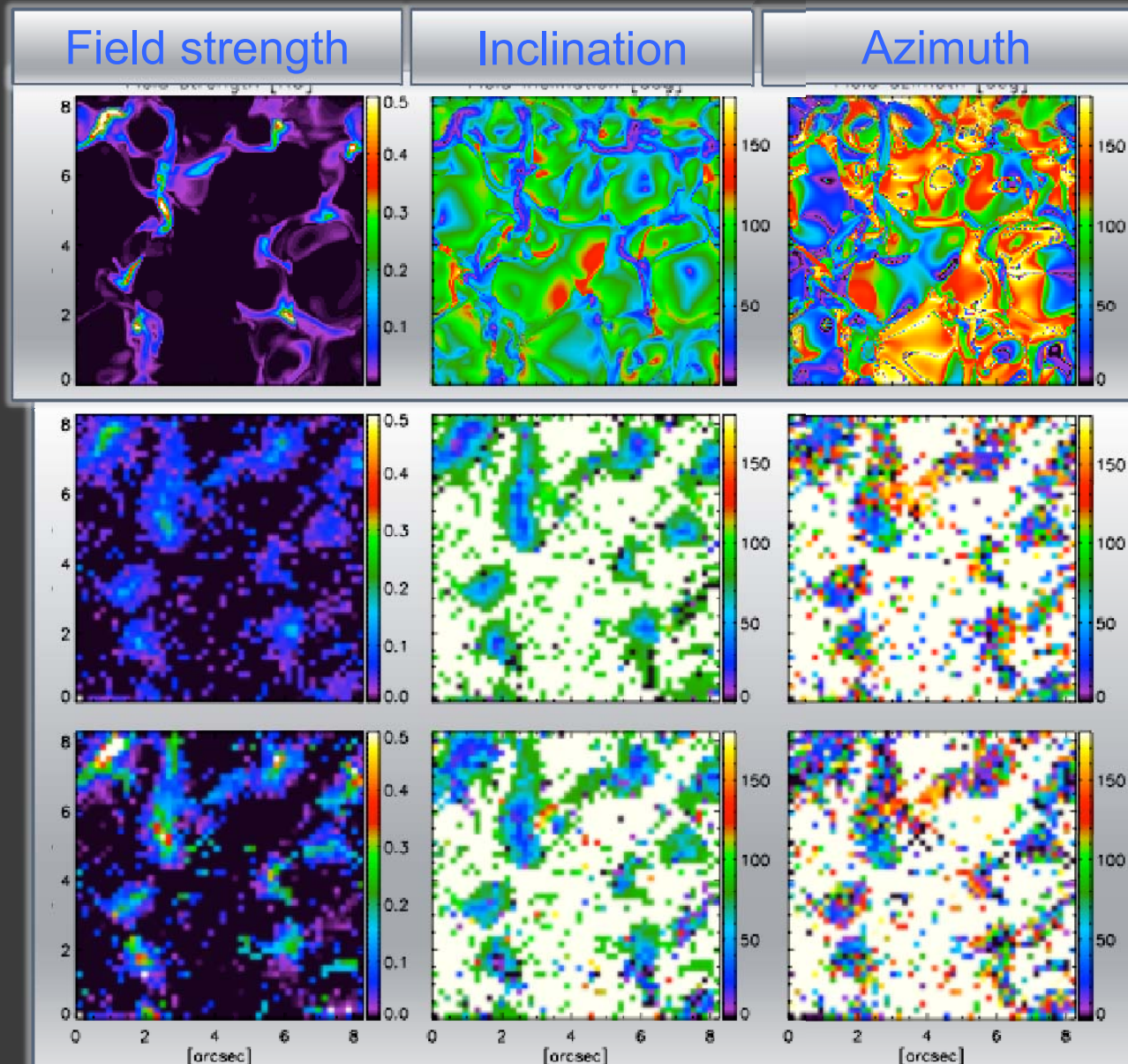
- average straylight profile calculated from Stokes I profiles in a 1'' wide box centered on the pixel
HeLix⁺: adjustable size of this box
- add this average profile to the Milne-Eddington profile using a straylight factor $\alpha = (1-f)$, f ... filling factor:

$$I = (1 - \alpha)I_m + \alpha I_{nm}$$

↙
→

magnetic component
(ME)
non-magnetic component
(straylight)

- straylight is interpreted as contamination (degradation of polarization signal due to diffraction).
- it might also represent magnetic filling factors smaller than one
 (more on that in the next minutes...)

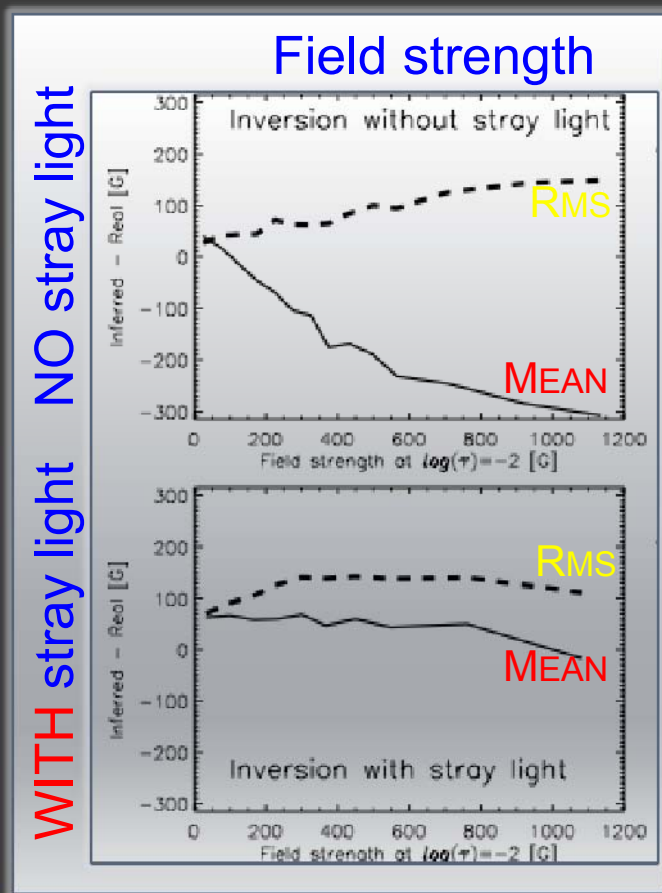


Real model stratification at $\log \tau = -2$

Results without using stray-light contamination

Results using local stray-light contamination

Mean and rms values of the errors defined as the difference between the inferred and the real parameters at optical depth $\log \tau = -2$.



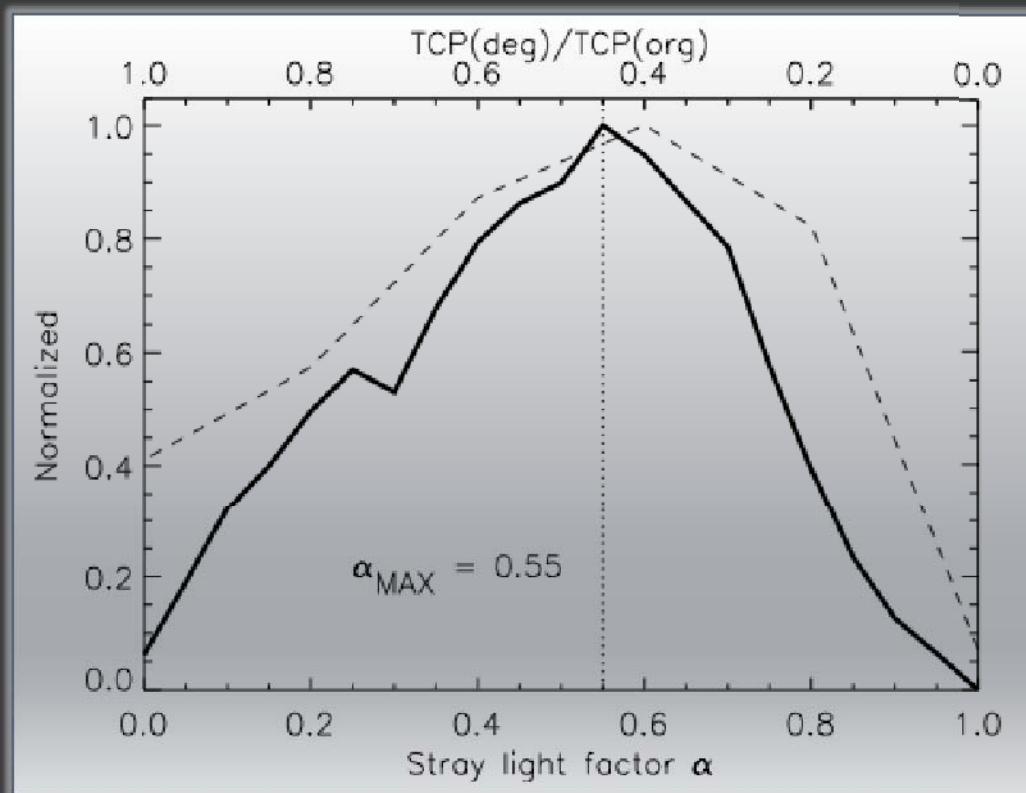
- Field strengths are underestimated if NO stray-light contamination is considered
- The inversion considering local stray-light contamination gives

Field strength error < 80 G

Field inclination error < 6°

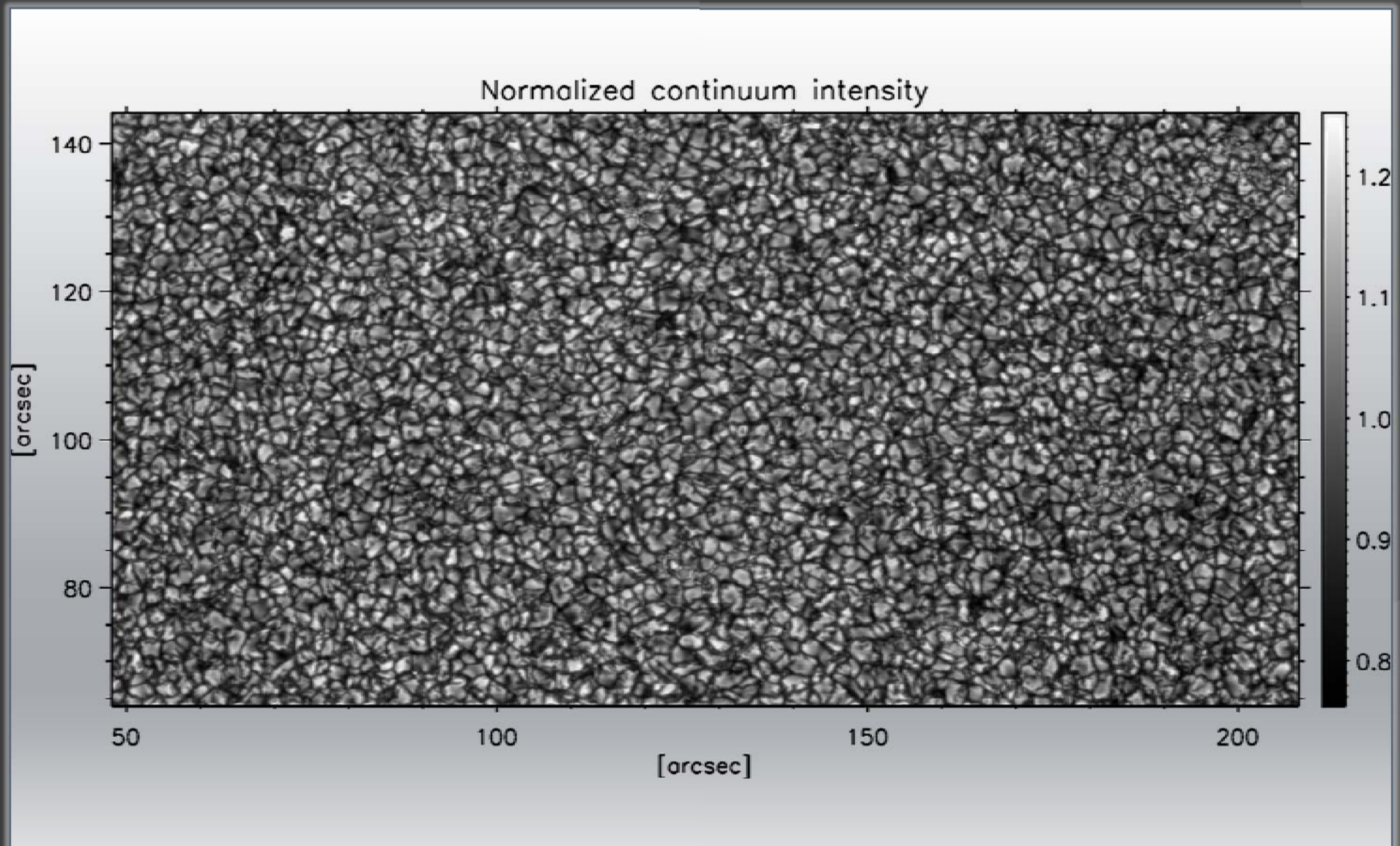
dashed: Histogram of stray-light factors derived from the inversion

solid: ratio of TCP in the degraded image with respect to that in the original image

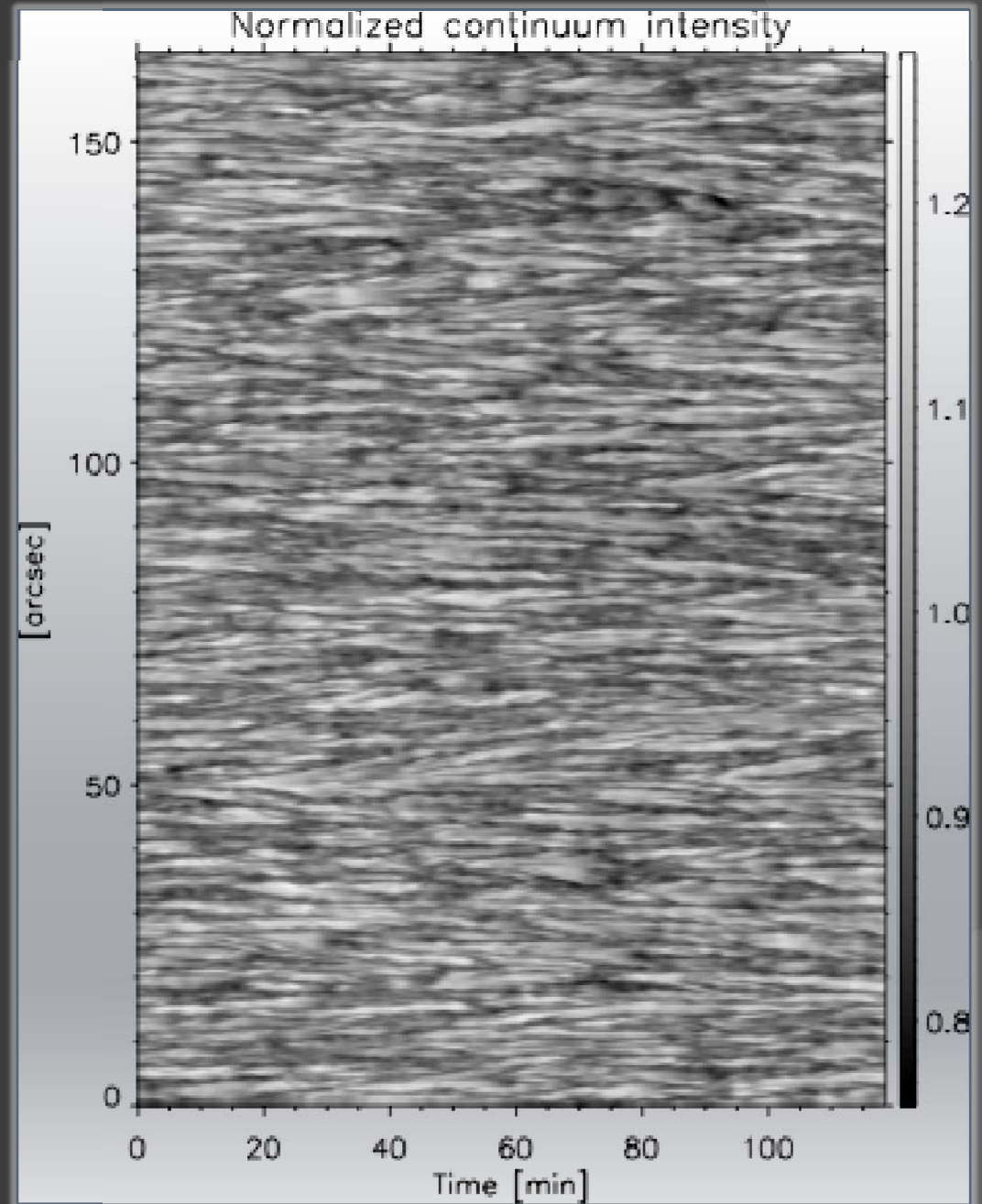


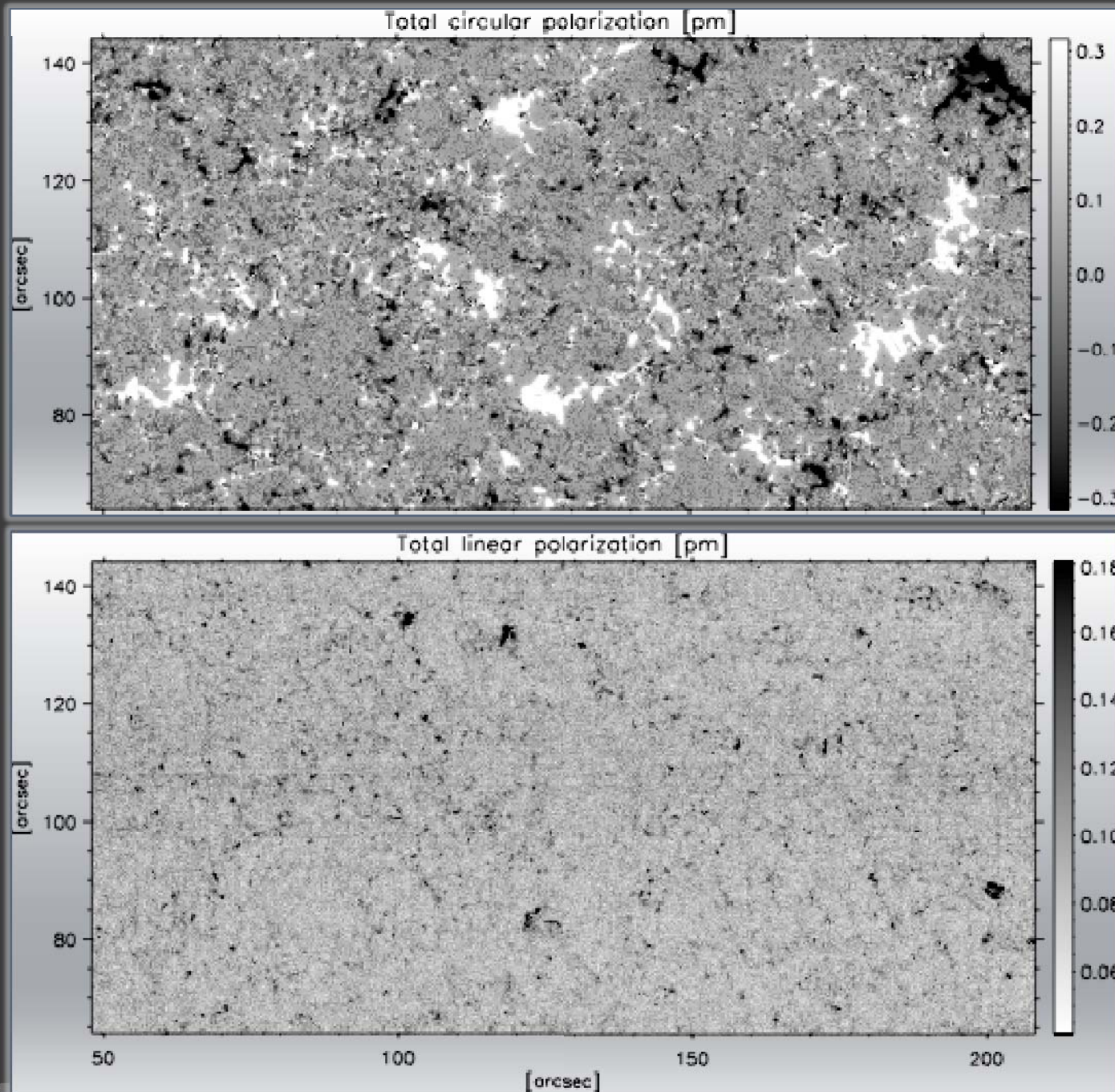
- The histogram has a **clear peak at 55%**
- There is a strong resemblance between the two distributions indicating that: **the stray-light factors derived from the inversion actually model the effects of telescope diffraction and CCD pixel size**
- The inferred α 's represent the **degradation of the instrument and NOT a real filling factor**

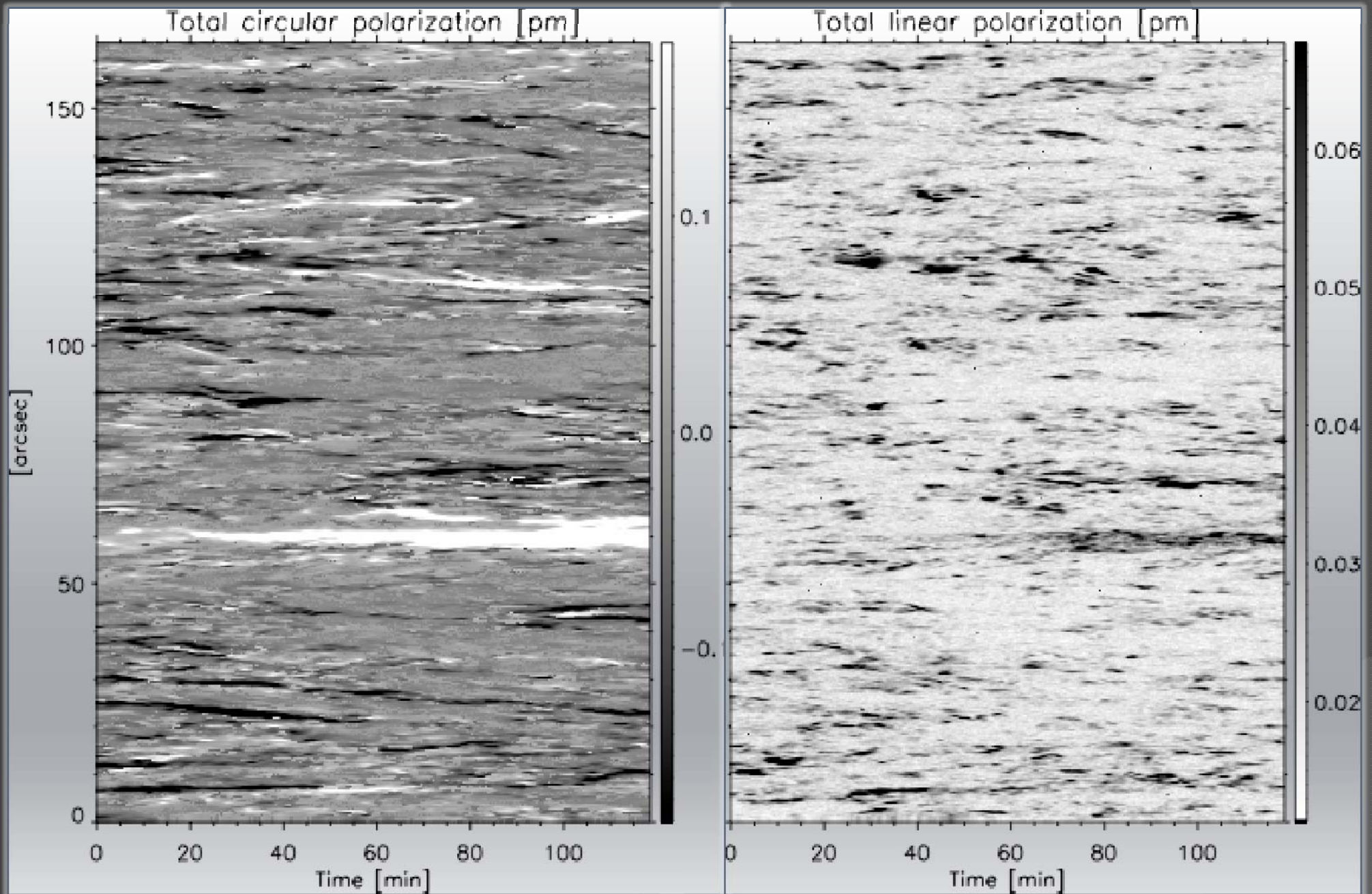
Normal map: 10 March, 2007
Exposure time of 4.6s per slit (noise level of $10^{-3} I_c$)



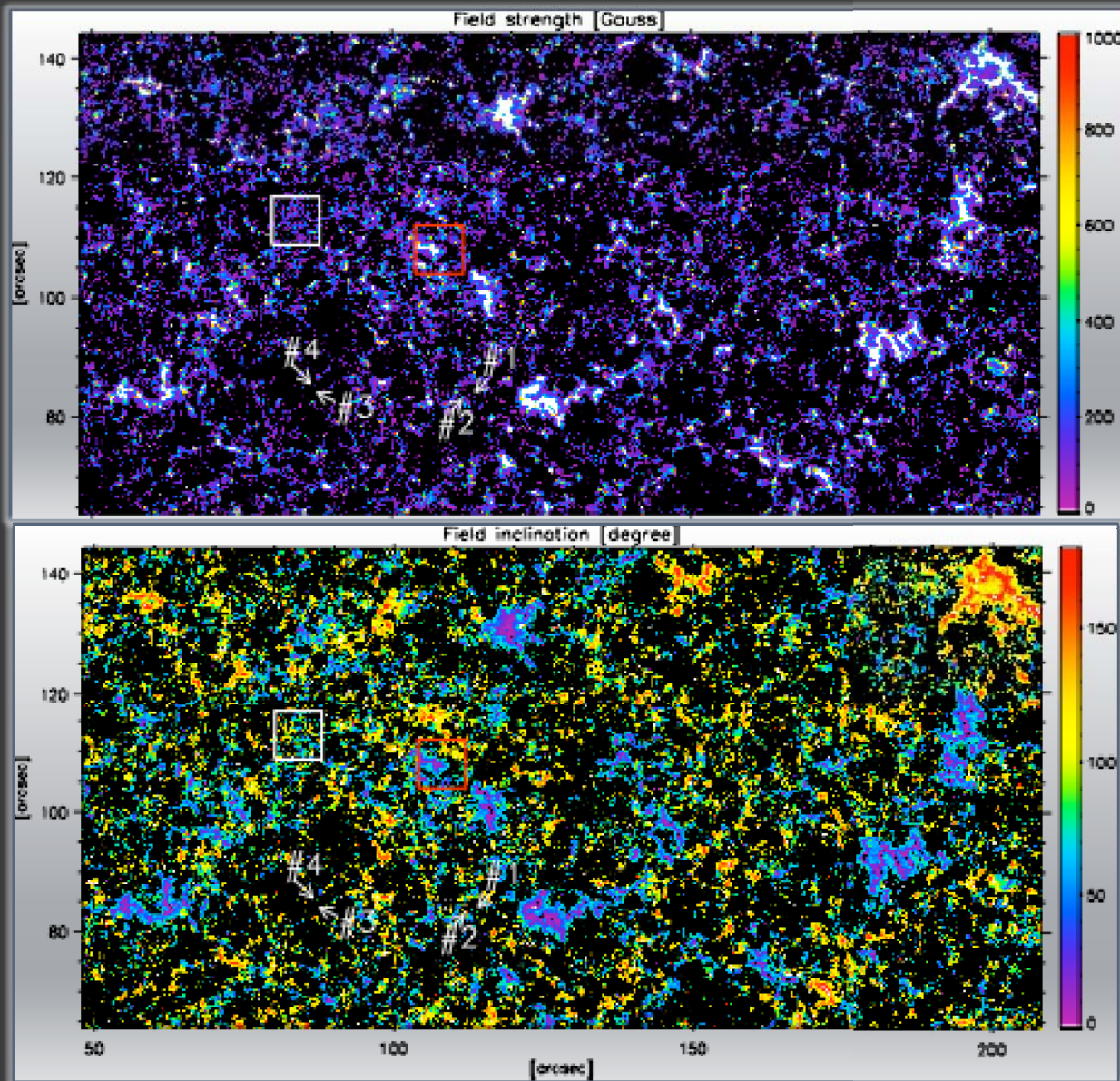
High S/N map: 27 February, 2007
Exposure time of ~ 60 s per slit
noise level of $3 \times 10^{-4} I_c$





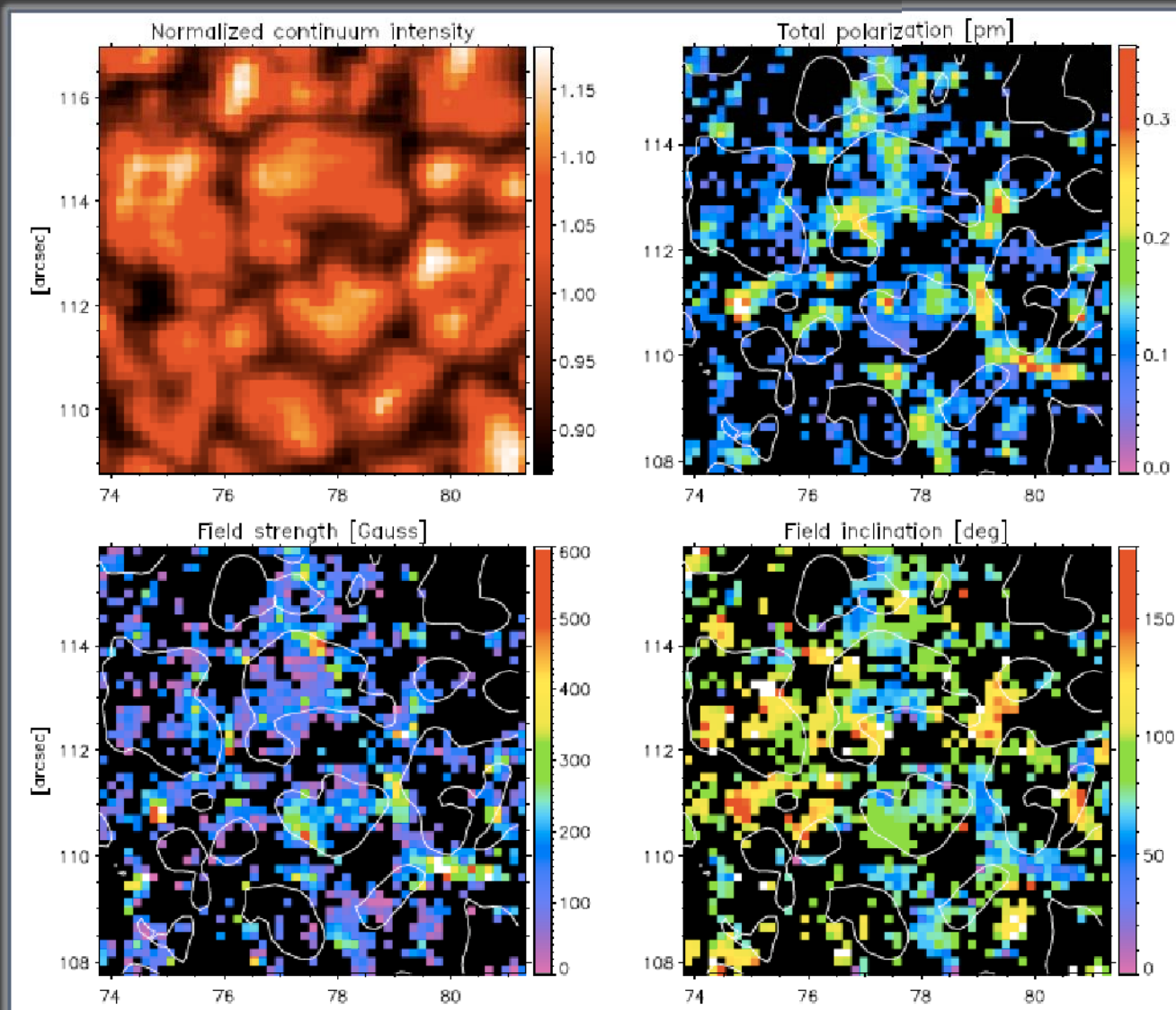


Inversion Results: Maps



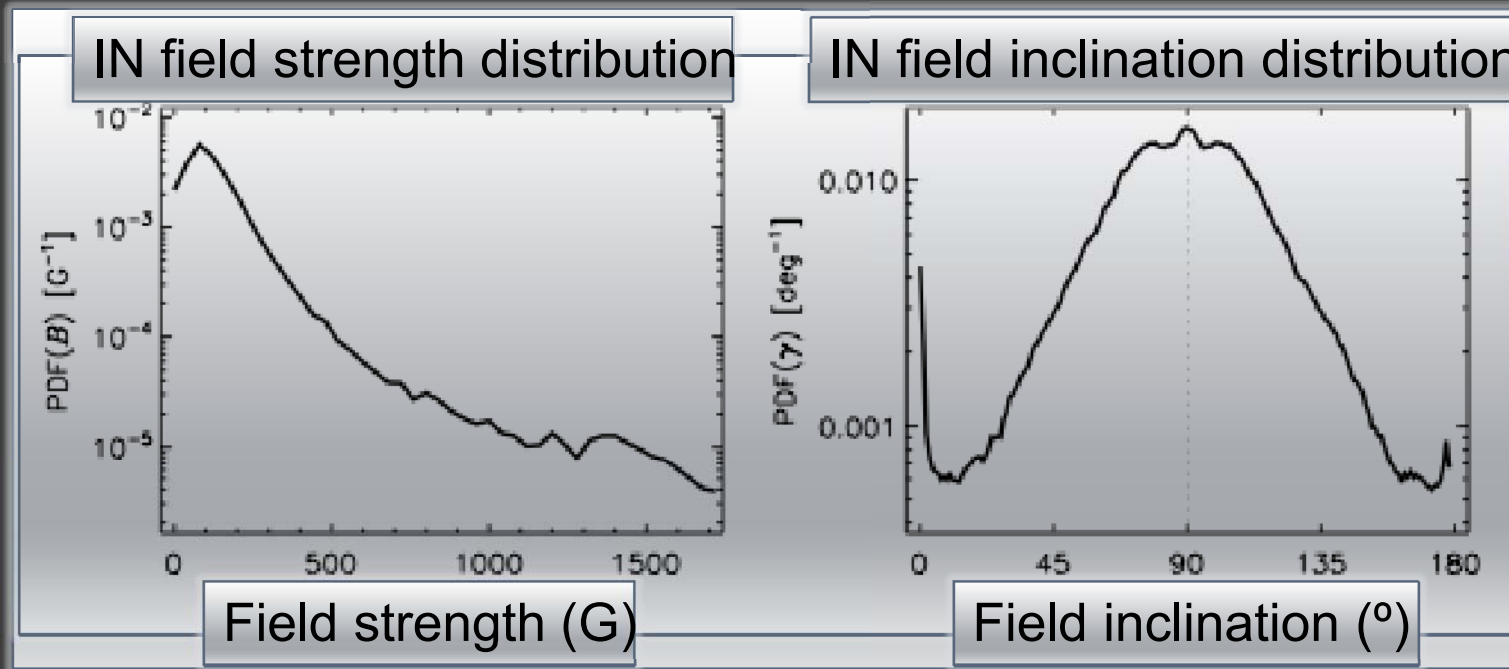
- The supergranular cells are clearly outlined by the network fields
- Network fields are characterized by strong field concentrations while the internetwork shows weaker fields
- The fields are more vertical in the network and more horizontal in the internetwork
- The stray-light factors are of the order of values of $\sim 60-80\%$ for the network and $70-90\%$ for the IN

Inversion Results: Maps



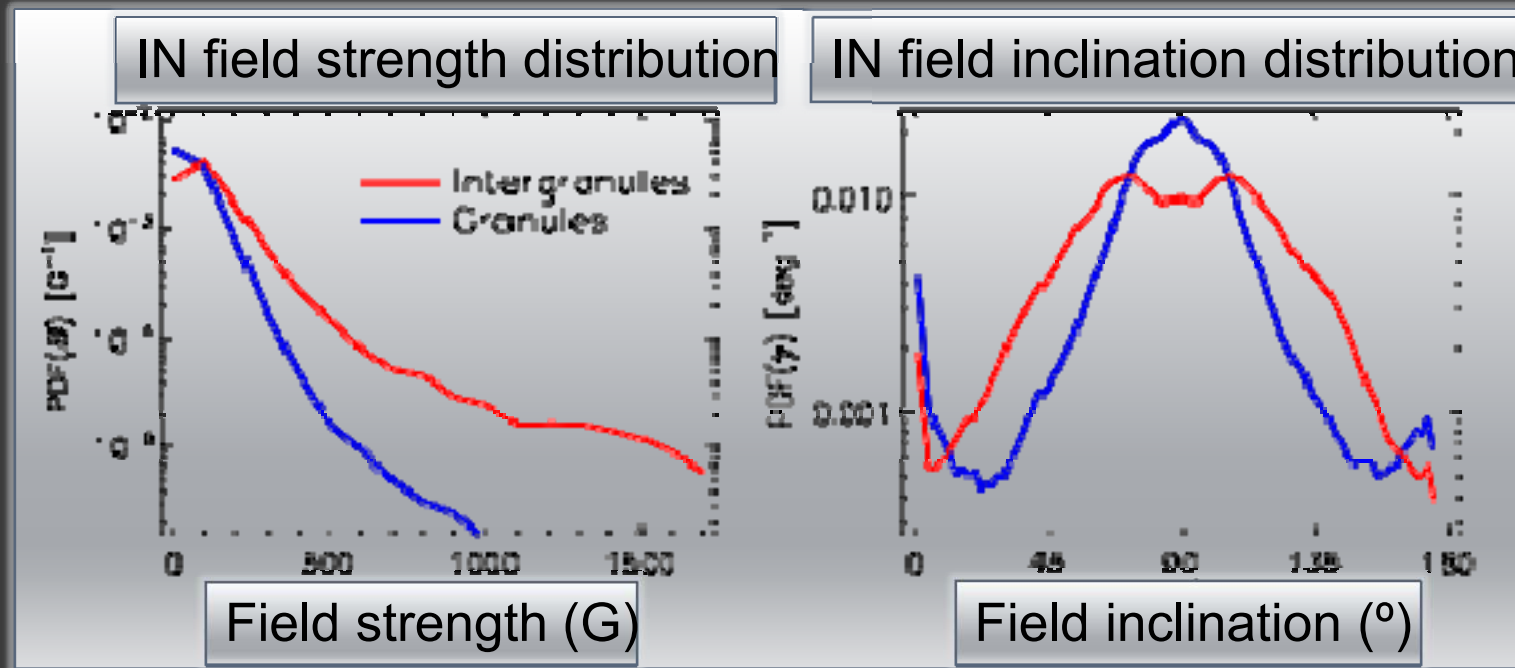
- The supergranular cells are clearly outlined by the network fields
- Network fields are characterized by strong field concentrations while the internetwork shows weaker fields
- The fields are more vertical in the network and more horizontal in the internetwork
- The stray-light factors are of the order of values of $\sim 60-80\%$ for the network and $70-90\%$ for the IN

Results: PDFs for B and INC



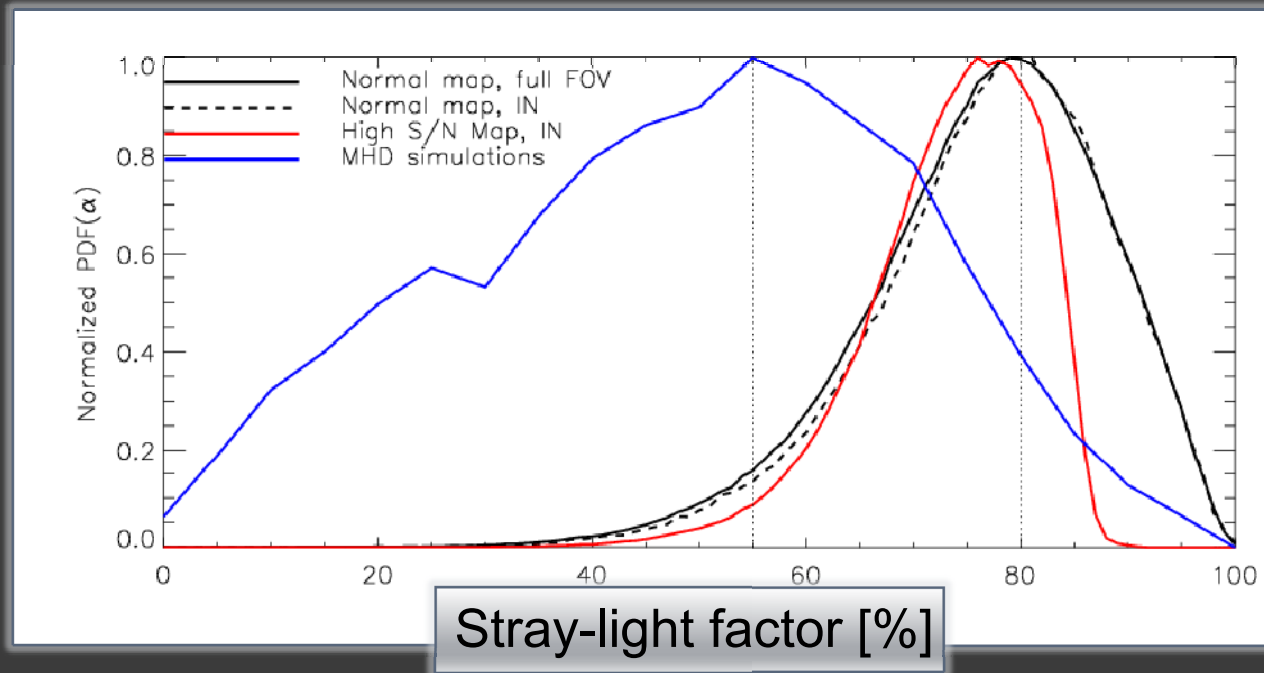
- The IN basically consists of hG flux concentrations
- The IN fields tend to be horizontally oriented
- The distribution of field strengths has a peak at 90 G and the inclination peaks at 90°
- These results are in agreement with the findings of Lites et al. (1996), Keller et al. (1994)
- They are in agreement with the results derived from infrared observations (Lin 1995, Lin & Rimmele 1999, Khomenko et al. 2003) and with the simultaneous inversion of visible and infrared lines (Martínez González et al. 2008)
- Notice that some fields tend also to be vertical

Results: Granular and intergranular fields



- 24% of the surface covered by granules in the IN contains magnetic flux detectable above the noise (in intergranules 28%)
- Strong fields are less abundant in granules
- There is a large fraction of very inclined fields in granules although vertical fields do also exist in granules

Results: Stray light factor contribution



- The distribution of stray-light factors peak at about $\sim 80\%$
- The stray-light factor is a combination of:
 1. Reduction of the polarization signals due to diffraction which would produce dilution factors of about 55%
 2. Real filling factor due to insufficient angular resolution
- The real magnetic filling factor is $f = (1-\alpha) / 0.45$
- This corresponds to an average filling factor $f \sim 45\%$, considerable larger than typical filling factors inferred from ground-based observations at 1"

Results: average fields and flux values

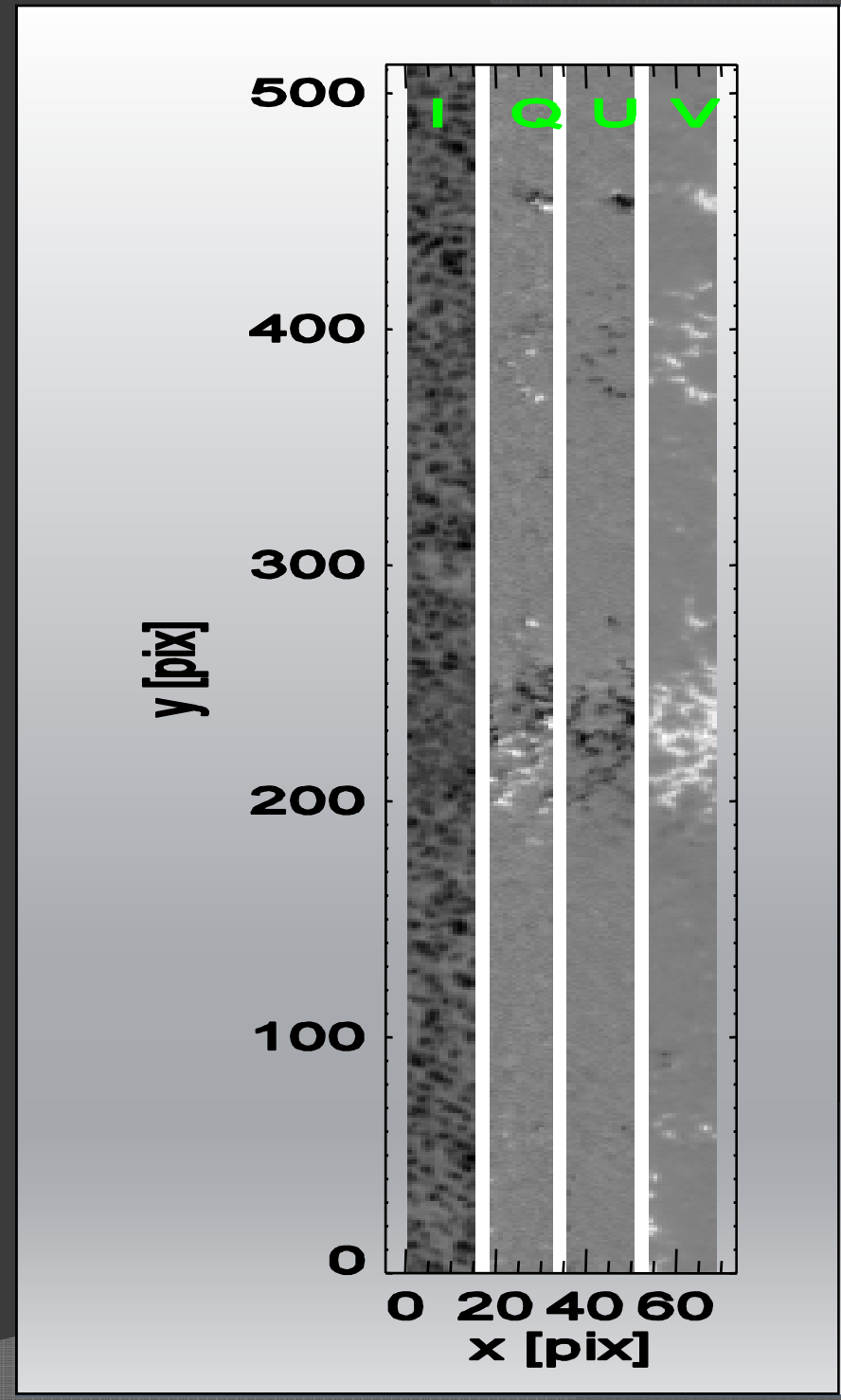
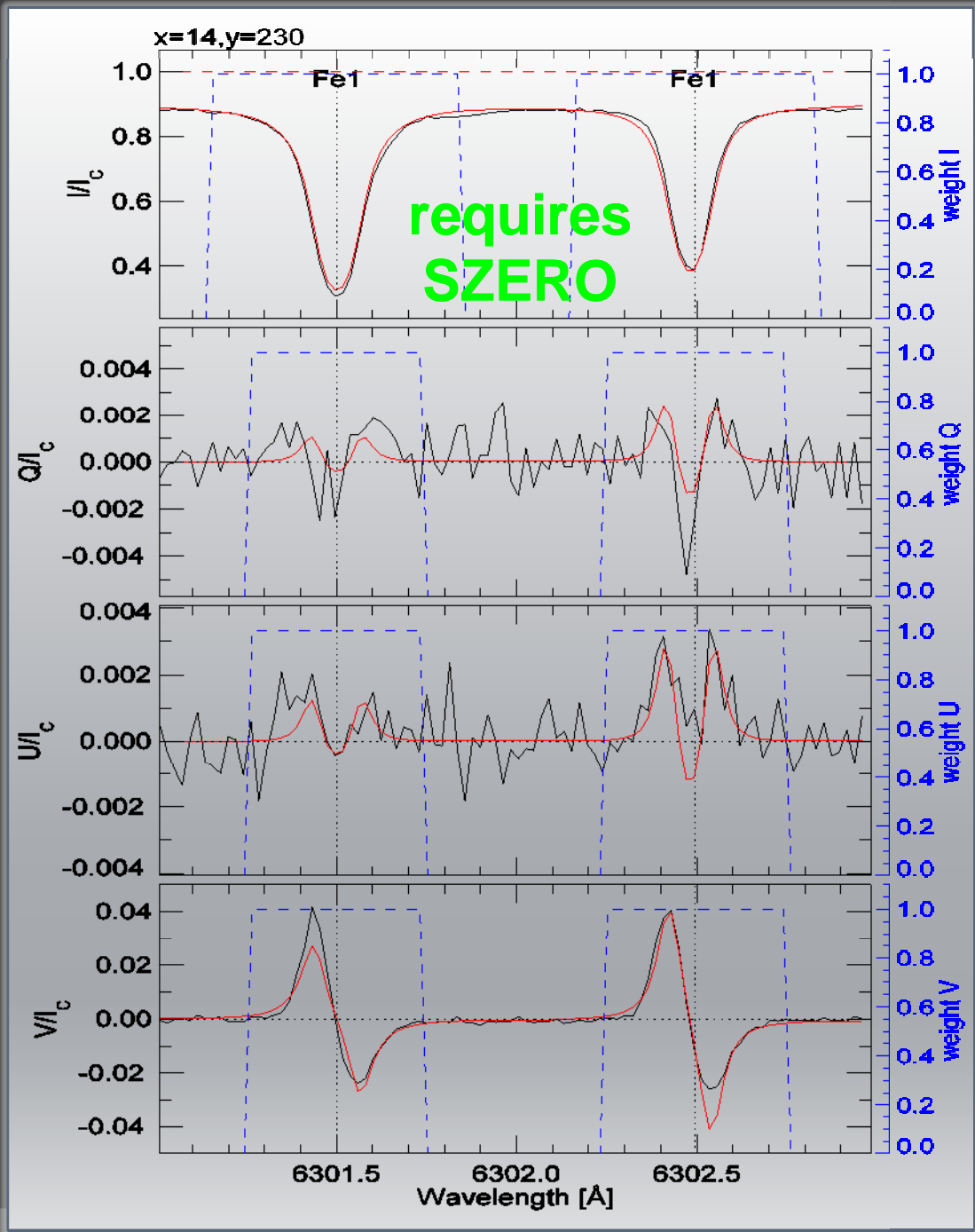
- Using the true magnetic filling factors and the high S/N data one can calculate the mean:
 - magnetic flux density $\bar{\Phi} = 25 \text{Mx cm}^{-2}$
 - average field strength $\langle \Phi \rangle = 125 \text{Mx cm}^{-2}$
- The flux density is of the same order of magnitude of previous estimates at lower spatial resolutions
- The flux imbalance is consistent with simulations (Steiner 2008)
- The average field strength is close to that obtained from Hanle measurements $\langle \Phi \rangle = 130 \text{Mx cm}^{-2}$ (Trujillo Bueno Shchukina, & Asensio Ramos 2004)

Conclusions: QS Hinode IN fields

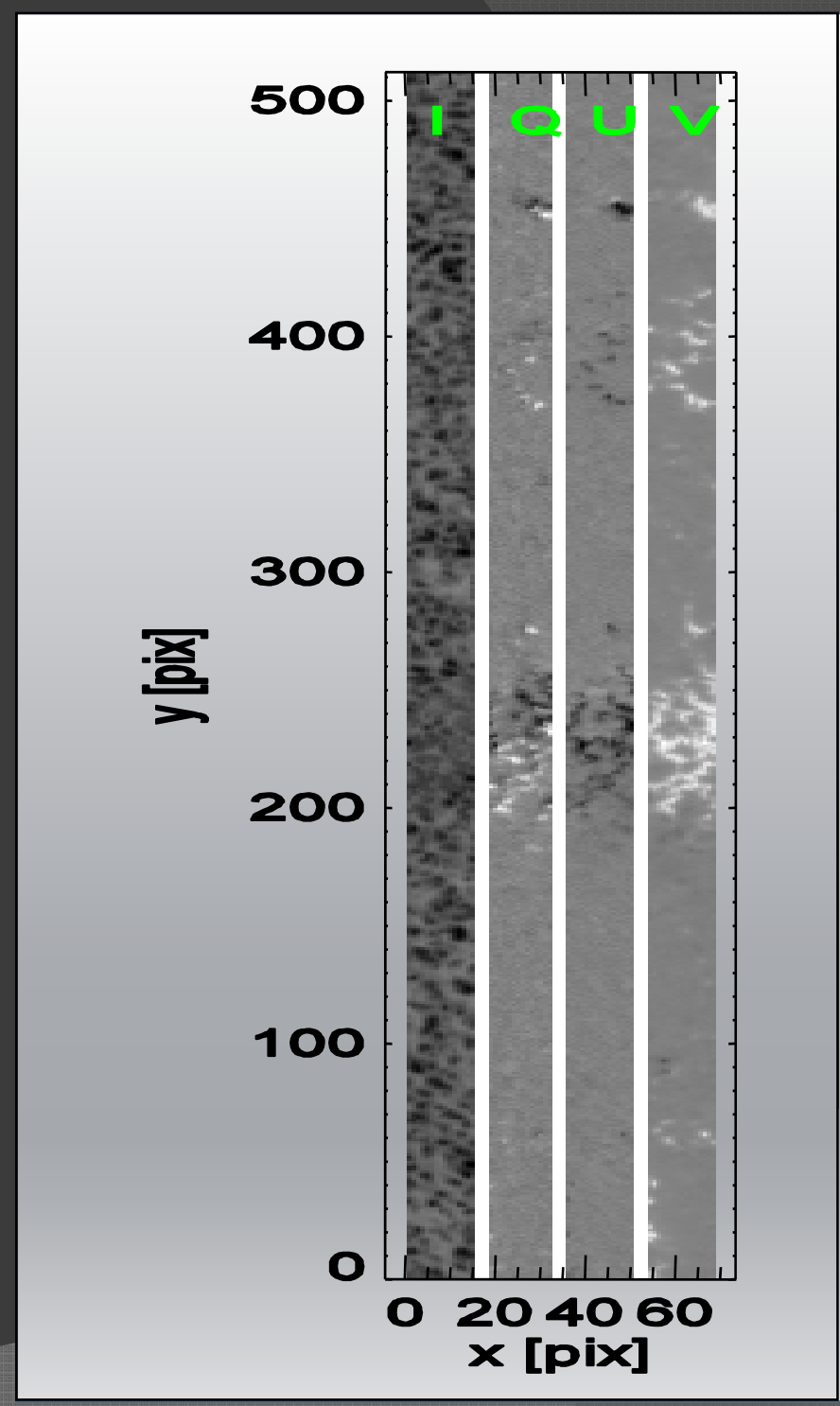
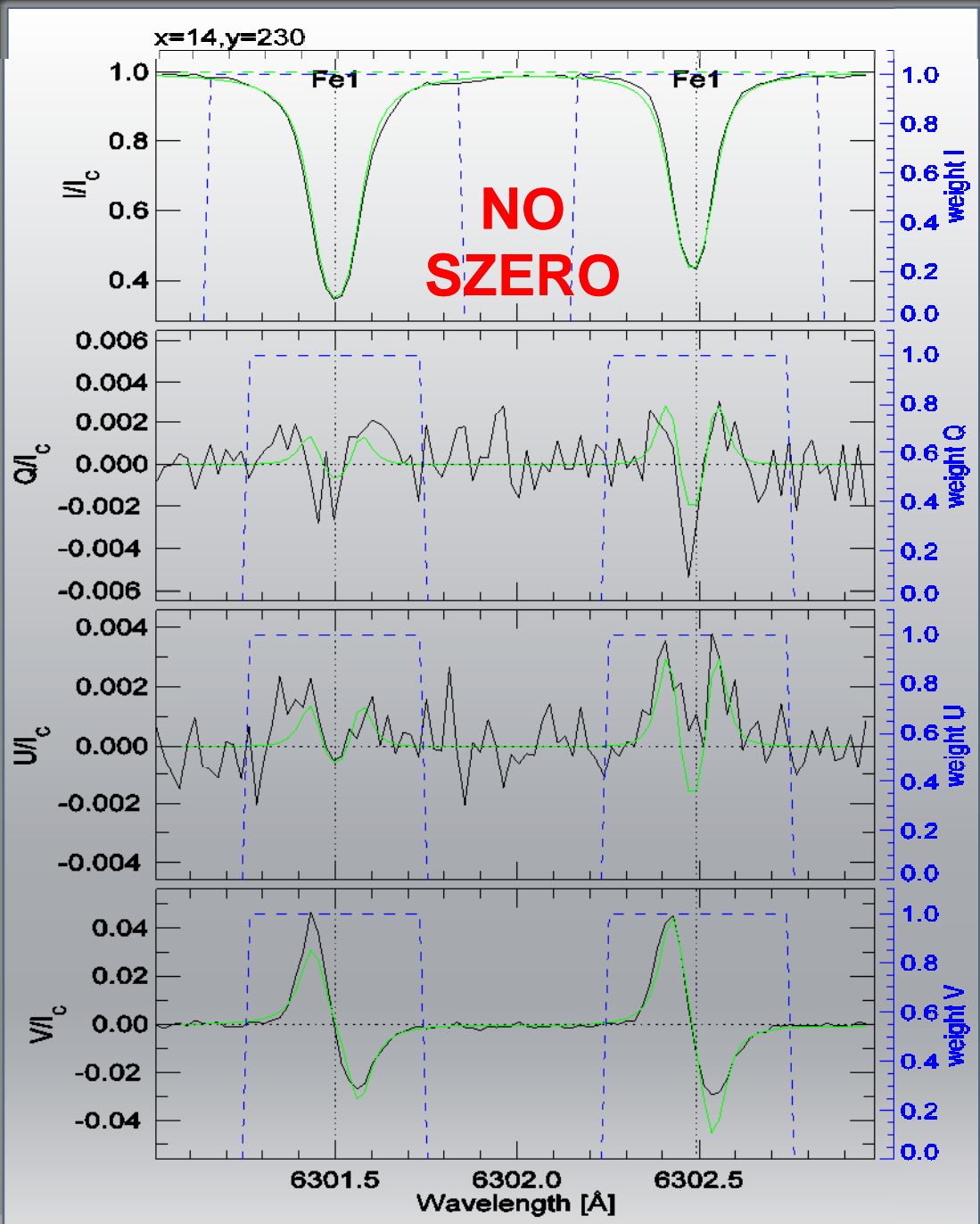
- The internetwork mostly consists in weak field concentrations.
 - *The average magnetic field strength is 125 Mx/cm^2*
 - *Hinode sees* the so-called “Hidden QS magnetism”
 - The reason is that inversions **are able** to determine the field strength and its filling factor **reliably**
(Orozco Suárez et al. (2009) to be submitted)
- There is still a discrepancy on the flux values and on the interpretation of the field inclinations distribution
 - We need better spatial resolution to fully resolve the magnetic structures **OR** to perform image deconvolution
 - SST/CRISP data, Sunrise IMaX

Exercise: inverting Hinode
data with HeI λ ⁺

Continuum normalization: IMAGE



Continuum normalization: LOCAL



Exercise III:

Potential problems with inversions



- read Hinode data
 - parameter crosstalk
SGRAD / ETA0
 - straylight: local/global
 - selection of atmospheric model
 - ambiguities
 - intrinsic (180° ambiguity)
 - Flux \leftrightarrow $B \cos(\gamma)$ FF
 - test convergence
 - small map
 - convolution (SST data?)
- LTE assumption
 - LS Coupling
 - ME approximation
 - ...

Required:
Experience!

Required:
Theoreticians